Zeitschrift: Schweizerische mineralogische und petrographische Mitteilungen = Bulletin suisse de minéralogie et pétrographie

Band: 85 (2005)

Heft: 2-3: Central Alps

Artikel: Apatite fission track ages from the Adula nappe : late-stage exhumation and relief evolution

Autor: Rahn, Meinert K.

DOI: https://doi.org/10.5169/seals-1662

Schweizerische Mineralogische und Petrographische Mitteilungen 85, 233–245, 2005

Apatite fission track ages from the Adula nappe: late-stage exhumation and relief evolution

Meinert K. Rahn[1,*]

Abstract

22 new apatite fission track (FT) ages from the Adula nappe are used to gain insight into the late-stage thermal and exhumation history of this tectonic unit and the adjacent Tambo nappe. Apatite FT ages vary from middle Miocene to Pliocene, with generally long track lengths and slightly skewed but otherwise narrow track length distributions.

The FT data do not show any horizontal gradient in exhumation, which would be compatible to a N–S tilting of the nappe such as may have been expected from the strong PT gradient found in the pre-Mesoalpine eclogite occurrences or from the Mesoalpine metamorphic gradient. Furthermore, no E–W tilting has been detected, such as could have been assumed as a result of late-stage updoming of the Lepontine dome to the west. Only the southernmost samples, close to the Insubric line, show relatively old ages (8–11 Ma), and track length data indicate continued fast exhumation close to the Insubric line up to that time. The area of youngest FT ages coincides with the highest pressure values as derived from Mesoalpine mineral assemblages, suggesting that the middle Adula nappe has undergone slightly increased exhumation and by this process has modified the present-day pressure contours of the eastern Lepontine dome.

Apatite FT ages along the sediment zone between Adula and overlying Tambo nappe (Misox zone) contrast with ages found at the Splügen sediment zone between Tambo and Suretta nappe further E. They are interpreted as the result of late-stage normal faulting between Adula and Tambo nappe with local heating of the Tambo nappe basis. A comparison between valley bottom samples in the Adula nappe reveals that the sampled valleys show distinct age patterns which illustrate the recent relief evolution and suggest that the Alpine water divide has moved to the N during the Miocene. Accordingly, the valley formation and its influence on the uppermost crustal isothermal planes have visibly influenced the apatite age pattern and provide an explanation for part of the scatter in apatite FT ages observed within the Adula nappe.

Keywords: Alps, Adula nappe, fission track, exhumation, late-stage evolution.

1. Introduction

The belt of Penninic rocks in the Central Alps is characterized by the presence of a prominent "dome" structure, the Lepontine dome, a strongly exhumed amalgamation of pre-Mesozoic crystalline basement nappes and separating thin zones of Mesozoic sedimentary rocks, both of which underwent amphibolite facies metamorphic overprint during the Alpine orogeny (Niggli, 1970; Frey and Ferreiro-Mählmann, 1999) at around 38 Ma (Steck and Hunziker, 1994). W and E of the Lepontine dome, the pattern of crystalline basement rocks, separated by thin sediment zones, extends into tectonic units of greenschist facies grade. The crystalline nappes to the E of the dome (Adula, Tambo and Suretta, from bottom to top) appear as isolated, N–S extending bodies and are separated from each other by zones of (a) deep water sediments (Bündnerschiefer, Fig. 1) in the Misox zone, and (b) a reduced sediment series from a former Mesozoic cover within the Splügen zone (Fig. 1a). The former nappe-covering sediments were mostly separated from their substratum. A number of sediment nappes of Northpenninic (e.g. Tomül, Grava nappes) and Middle Penninic origin (e.g. Schams nappes) are thought to represent Mesozoic sediments which were originally sedimented S of the Adula nappe (Steinmann, 1994) or on top of the Tambo and/or Suretta nappe (Schmid et al., 1990). The Adula nappe is thought to represent the southernmost crystalline

[1] Mineralogisch-Geochemisches Institut, Albert-Ludwigs-Universität Freiburg, 79104 Freiburg, Germany.
* Present Address: Swiss Federal Nuclear Safety Inspectorate, 5232 Villigen-HSK, Switzerland.
<meinert.rahn@hsk.ch>

0036-7699/05/0085/233

rocks of the Eurasian plate, while the Tambo and Suretta nappes are thought to be the former crystalline basement of the Briançonnais, which formed a horst structure between a marginal ocean basin (Valaisan trough) to the N and an open ocean to the S (Schmid et al., 1990). Accordingly, the deep-water sediments in-between the Adula and Tambo nappe (Misox zone) contain only minor remnants of oceanic crust, while the Tambo nappe was covered by shallow-water sediments, and major segments of deep-water sediments and oceanic crust are found at the top and to the E of the Suretta nappe (Avers schists, Malenco serpentinites).

Among the nappes E of the Lepontine dome, the Adula nappe has the largest N–S extension and is the only unit that contains rocks of Alpine greenschist to granulite facies metamorphic grade (Frey and Ferreiro-Mählmann, 1999; Bucher-Nurminen and Droop, 1983). Prior to its Barrovian

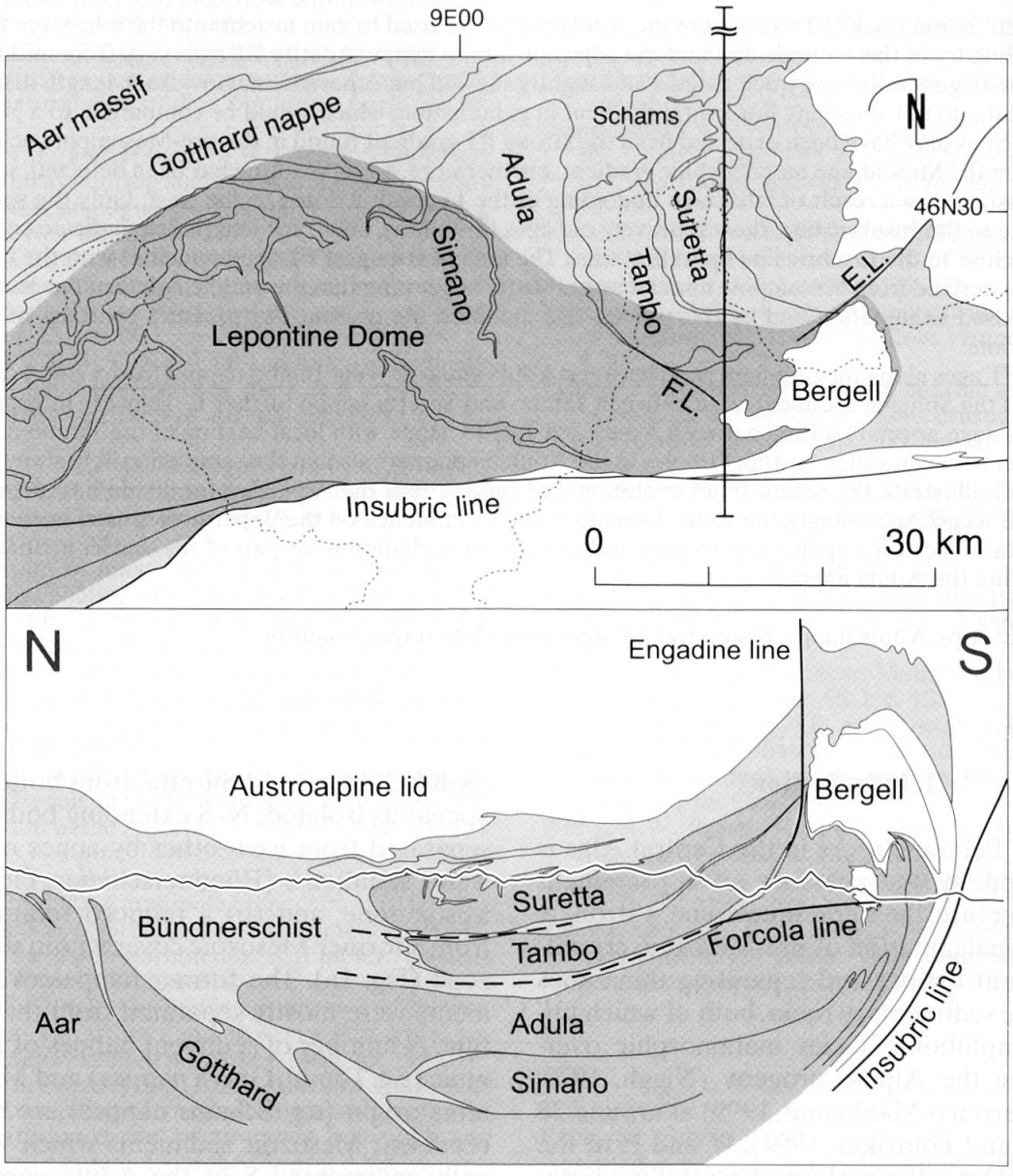

Fig. 1 (a) Overview of tectonic units of the Central Alps with outline of the Tertiary amphibolite facies metamorphic Lepontine dome (dark grey) and the Mesoalpine greenschist facies areas (light grey). Tectonic units showing subgreenschist facies overprint (Southern Alps), a Cretaceous metamorphic overprint (Austroalpine units), or late- to post-metamorphic intrusive age (Bergell) are white in colour. The location of the cross section in Figure b is indicated by a thick black line. E.L. — Engadine line, F.L. — Forcola line. (b) N–S cross section perpendicular to the regional Alpine strike, based on deep-seismic data (Schmid et al., 1996), showing the sequence of crystalline nappes (Adula, Tambo and Suretta) and interlayered sediment zones, and their structural relationship to the Bergell intrusion. Crystalline nappes are shown in dark grey, sedimentary rocks (and remnants of oceanic crust) in light grey. Note the horizontal northern and central parts of the Adula nappe, and its sharp down-bend in the southern part (projected into the air).

metamorphic overprint, the Adula nappe was part of a south-dipping subduction zone and underwent eclogite facies conditions (e.g. Heinrich, 1986; Meyre et al., 1997; Dale and Holland, 2003), which is illustrated by numerous eclogite occurrences found mostly along its eastern margin, but also by the presence of ultramafic lenses, surrounded by eclogites in the HT metamorphic Mergoscia-Arbedo zone. Preliminary age dating (Becker, 1993) suggests an Eocene age for the eclogite formation. Calculated PT conditions for the eclogites and the two ultramafic lenses at Cima di Gagnone and Alpe Arami show a systematic increase in pressure and temperature from N to S, suggesting that prior to the Barrovian overprint the Adula unit may have become a coherent nappe within a 45° S-verging subduction zone (Dale and Holland, 2003). Derived metamorphic conditions (Meyre et al., 1997; Dale and Holland, 2003) reveal a clockwise PT-evolution with strong exhumation of the Adula nappe after the pressure maximum. Under the assumption of coherence of the Adula nappe crystalline body, established PT paths were used to develop a model, in which the Adula nappe is proposed to have acted as a "melon pit" which was extruded along the subduction channel (Engi et al., 2001; Roselle et al., 2002) back to a mid-crustal position, where the Adula unit subsequently underwent a Barrovian overprint as a result of continent-continent collision (Engi et al., 2001).

To the W of the Lepontine dome, a major fault zone, the Simplon Fault (Mancktelow, 1992) represents an important element for the exhumation of the dome and its amphibolite facies rocks (Steck and Hunziker, 1994). To the E of the dome, there is no such prominent tectonic feature, but rather a number of faults such as the Turba mylonite zone (Nievergelt et al., 1996) which recorded post-metamorphic normal movements. Meyre et al. (1998) and Schlunegger and Willett (1999) proposed that the Forcola zone represents an eastern equivalent to the Simplon Fault, having taken up similar amounts of syn-orogenic extension. The Forcola line represents the southward extension of the Misox zone and S of the Forcola pass forms the nappe separating tectonic element between Adula and Tambo nappe, but then separates the Gruf complex (containing granulite-facies relics) from the rest of the Adula nappe (Meyre et al., 1998). Close to the Forcola pass, the Forcola line is dipping some 40 to 50° towards NE. Tilting of the units is supported by the fact that the Adula, Tambo and Suretta nappes show a marked inclination to the ENE. The suggestion that the Forcola zone represents an easterly equivalent to the Simplon fault gains further support by the fact that the time of normal faulting at the Forcola zone (Forcola phase, 21–18 Ma, Meyre et al., 1998) coincides with the period of main activity at the Simplon fault (at around 18 Ma, Grasemann and Mancktelow, 1993). However, FT ages from the Forcola fault close to the Novate granite indicate no large vertical offset along this plane younger than about 20 Ma (Ciancaleoni et al., 2001), while for the Simplon fault, extensional movements are supposed to have continued to recent times (Steck and Hunziker, 1994).

The role of the Simplon fault zone was illustrated by a combination of structural observations (Mancktelow, 1992; Steck and Hunziker, 1994), FT data (Wagner et al., 1977) and thermal modelling for the Simplon Fault (Grasemann and Mancktelow, 1993). Offset metamorphic isograds have been mapped across the Simplon Fault, but not at the eastern margin of the dome (Frey and Ferreiro-Mählmann, 1999). This suggests that the exhumation of the Lepontine dome at its western margin is mostly the result of extensive normal faulting; to its E, however, exhumation is suggested to be the result of more local doming, large-scale tilting and restricted normal faulting along several nappe-separating sediment zones (i.e. the Misox and Splügen zone) within the nappe stack of Penninic and Austroalpine units (Nievergelt et al., 1996).

To the S, the main Adula crystalline nappe body bends E and towards the Bergell intrusion, which itself has undergone strong exhumation after magmatic emplacement (Wagner et al., 1979; Giger and Hurford, 1989; Berger et al., 1996). Exhumation, together with backthrusting is thought to have taken place in connection with differential movements along the Insubric line in the late Oligocene and ceased by 19 Ma (Hurford, 1986). In present-day N–S cross sections, the Adula nappe occurs as a flat lying body with a thickened frontal part and its southern end bent upwards towards the Bergell intrusion (Fig. 1b). In E–W direction the crystalline body and its main schistosity are inclined by 20° to the ENE (Jenny et al., 1923).

In this study, the N–S extending part of the Adula crystalline nappe body is characterized by apatite FT dating in order to investigate whether the late-stage cooling of the nappe shows evidence of (a) tilting after the strongly inclined position of the nappe within the subduction channel (Engi et al., 2001), (b) tilting leading to the present-day metamorphic gradient from high-grade amphibolite facies in the S to medium-grade greenschist facies at the northern front (Todd and Engi, 1997), (c) tilting during exhumation of the high grade metamorphic Lepontine dome to the W

(Steck and Hunziker, 1994), or (d) tilting due to backthrusting along the Insubric line. In addition, the possible effect of the relief on the closure of the apatite FT system is investigated by looking at samples from major river valleys with and without evidence for a structurally related origin.

2. Sample processing and results

17 samples were collected for FT analysis along the N–S and E–W extension of the Adula crystalline nappe N and W of the Mesolcina valley (Table 1, Fig. 2). One sample was taken from Alpe

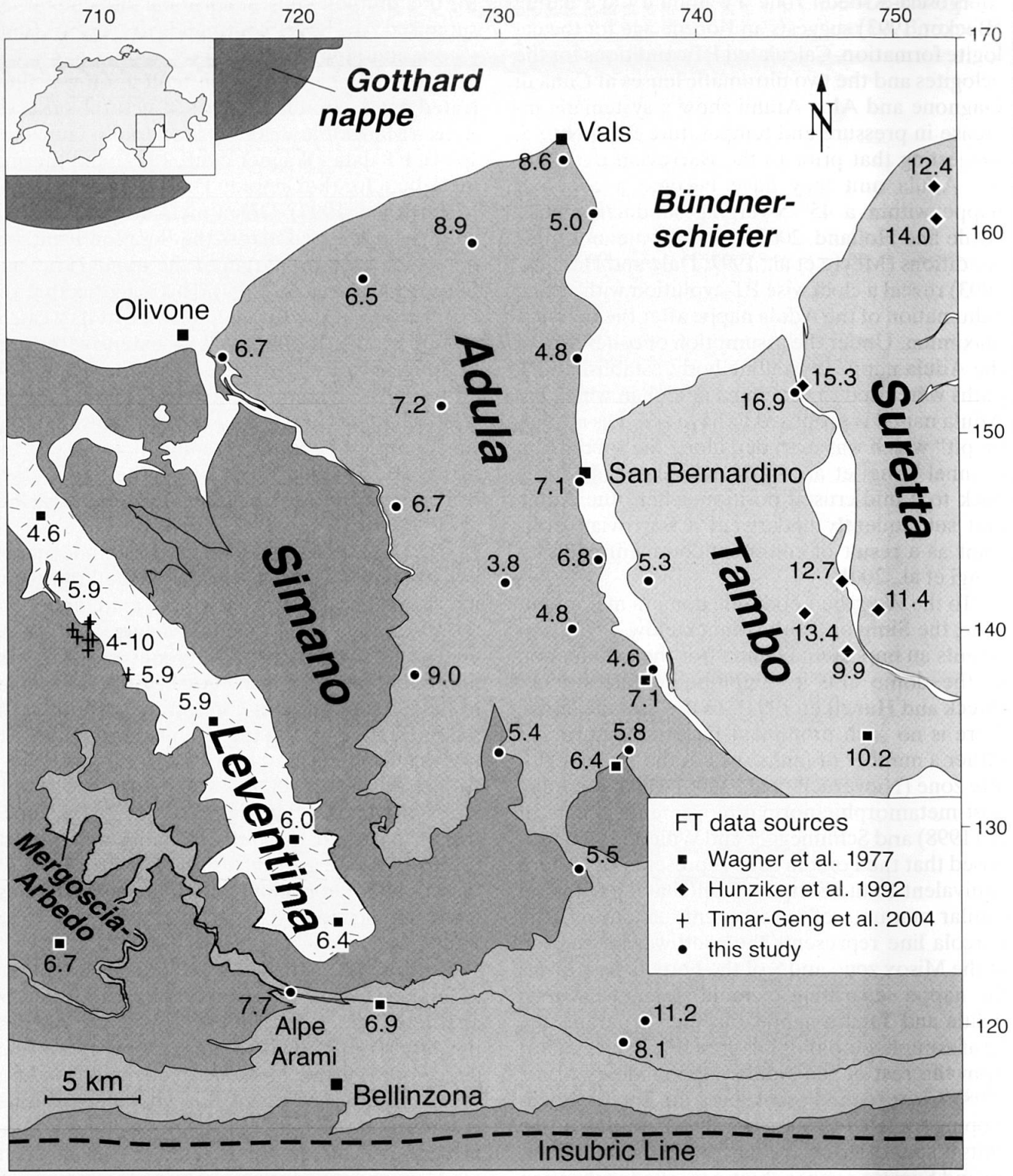

Fig. 2 Sample localities and apatite fission track ages from the Adula nappe and neighbouring tectonic units; data from Wagner et al. (1977), Hunziker et al. (1992), Timar-Geng et al. (2004), and this study. The longitude and latitude values correspond to km in the Swiss coordinate net. For age errors, see Table 2. Outlines of tectonic units from Berger et al. (2005).

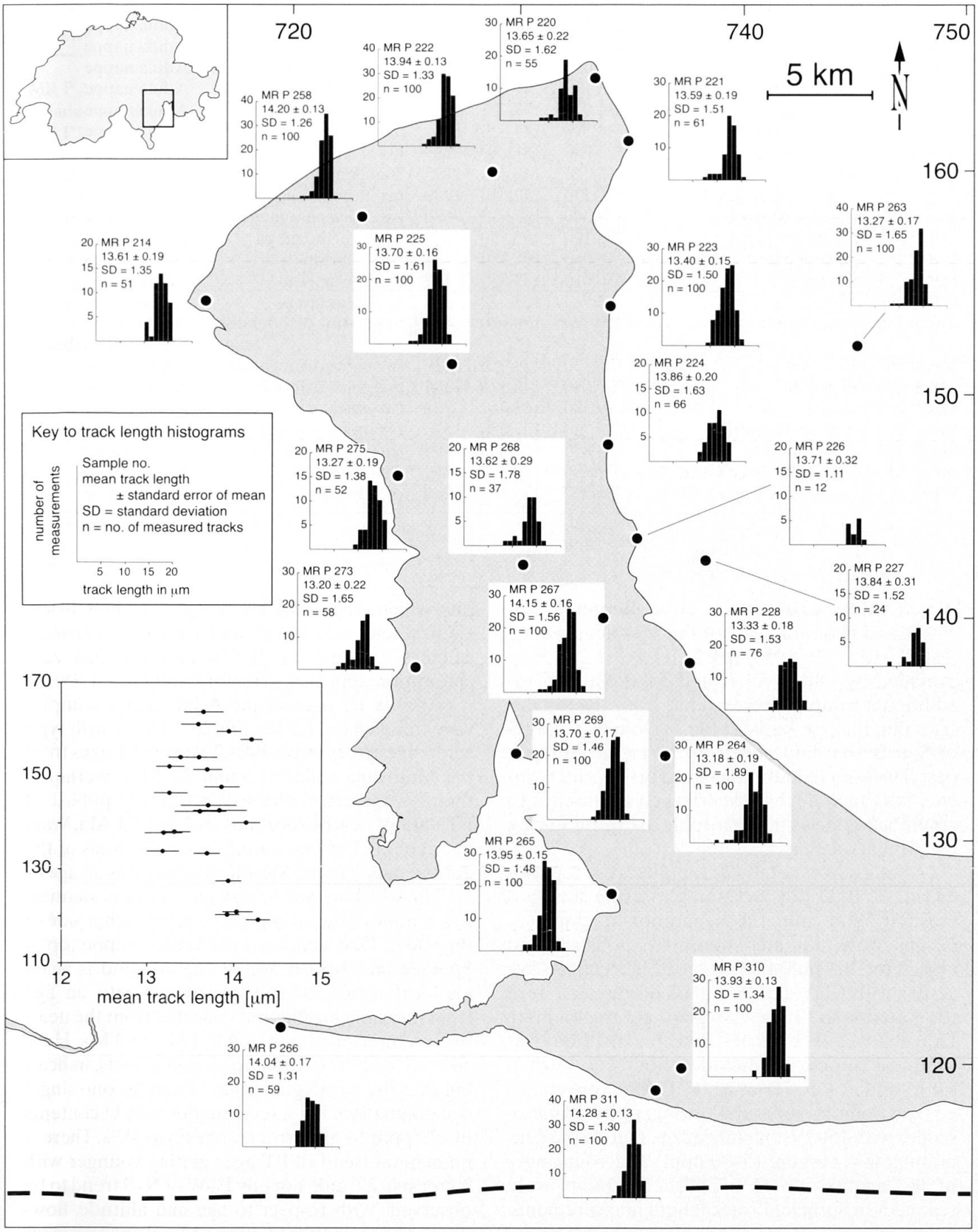

Fig. 3 Apatite fission track length data from the Adula nappe and adjacent units. The inset shows the N–S distribution of the mean track length values (± 1 standard error of the mean). Outlines of the Adula unit from Berger et al. (2005).

Table 1 Location and lithological characterization of the Adula and Tambo nappe fission track samples. Indicated x and y coordinates correspond to the Swiss coordinate net (units: km).

Sample Nr.	locality	length	width	altitude	lithology	tectonic unit
MR P 214	Solario	716.050	153.840	1150	bt orthogneiss	Adula nappe
MR P 220	Vals	733.375	163.740	1300	sericite gneiss	Adula nappe
MR P 221	Peil	735.010	161.100	1665	ser chl orthogneiss	Adula nappe
MR P 222	Guraletsch	728.730	159.600	1905	ms orthogneiss	Adula nappe
MR P 223	Hinterrhein	734.075	153.775	1650	ms augen gneiss	Adula nappe
MR P 224	San Bernardino	734.190	147.525	1660	ms gneiss	Adula nappe
MR P 225	Zapporthütte	727.020	151.250	2285	ms orthogneiss	Adula nappe
MR P 226	Spina	735.720	143.520	1195	fs-augen paragneiss	Adula nappe
MR P 227	Pian San Giacomo	738.230	142.510	1280	ms-bt-chl paragneiss	Tambo nappe
MR P 228	Castello Mesocco	738.060	137.970	680	two mica paragneiss	Adula nappe
MR P 258	Lampertschalp	723.190	157.750	2080	augen orthogneiss	Adula nappe
MR P 263	Splügenpass	745.060	151.980	2120	very fine gneiss	Tambo nappe
MR P 264	Soazza	736.610	133.850	470	light ms gneiss	Adula nappe
MR P 265	Norantola	733.580	127.430	375	two-mica gneiss	Adula nappe
MR P 266	Alpe Arami	719.390	120.970	1445	migmatitic orthogneiss	Adula nappe (zone of Mergoscia-Arbedo)
MR P 267	Trescolmen	733.730	139.950	2110	two-mica orthogneiss	Adula nappe
MR P 268	Pian d'As	730.230	142.370	1385	two-mica orthogneiss	Adula nappe
MR P 269	Cauco	729.380	133.440	980	two-mica orthogneiss	Adula nappe
MR P 273	Alpe di Lesgiüna	725.720	137.680	1530	two-mica orthogneiss	Adula nappe
MR P 275	Alpe di Piotta	724.890	146.240	1995	(bt)-ms orthogneiss	Adula nappe
MR P 310	Sass della Vacca = Mu 1053	737.370	120.155	2290	paragneiss	Adula nappe
MR P 311	Cima della Stagn = OJ 28	736.200	119.150	2280	orthogneiss	Adula nappe

Arami (Mergoscia-Arbedo zone, Berger et al., 2005), and two samples S of the Mesolcina valley (MRP 310 = Mu 1053, MRP 311 = OJ 28) were provided by Oliver Jeker and Josef Mullis. Two additional samples were added from the Tambo crystalline nappe basis in the Mesolcina valley S of San Bernardino and from its top at Splügen pass. The sampled lithologies are ortho- and paragneisses (Table 1) that experienced greenschist to amphibolite facies metamorphic overprint during the Alpine orogeny.

Apatites from totally 22 samples were separated out of 10–20 kg rock samples using standard crushing and mineral separation techniques. Grains were mounted in epoxy, polished and etched for 20 s in 5M HNO_3 at 20 °C. Samples, together with CN5 standard glass dosimeters, were irradiated in the TRIGA reactor at Oregon State University. The external detector method was used and muscovite mica detectors were etched for 45 min in 40% HF at 20 °C. Tracks were counted and lengths measured using optical microscopes with 1600× magnification. Due to the generally low U content (5–70 ppm) and young ages of the apatites up to 3 polished mounts were scanned for sufficient track length measurements. Compositional effects on the closure temperature of the apatite FT system were avoided by not counting on grains with fat tracks, i.e. large etch pits, which commonly are assigned to be Cl-rich. Central ages (Galbraith and Laslett, 1993) were calculated using the IUGS-recommended zeta calibration approach (Hurford and Green, 1983).

Apatite FT ages of the Adula nappe samples vary from 3.8 to 11.2 Ma (Table 2, Fig. 2) with typical 1σ age errors of 10–20%. Two new FT ages from the Mesolcina valley (4.9 and 5.8 Ma) overlap in their 2σ age error with two previously published FT data of nearby localities (6.4 and 7.1 Ma, Wagner et al., 1977). One sample from the basis of the Tambo nappe in the Mesolcina valley has an age of 5.3 Ma, which within 2σ statistical error is identical to a sample of the Adula nappe on the other side of the valley. One sample of the Tambo nappe top at Splügen pass has an age of 16.9 Ma and is again identical within 2σ statistical error with an age from the same locality, but collected from the nearby Suretta nappe basis (KAW 1240, 15.3 Ma, Hunziker et al., 1992). All samples pass χ^2 tests, indicating that the single grain ages belong to one single age population. For a few samples with U contents of <10 ppm 1σ age errors range up to 35%. There is no general trend of FT ages getting younger with increasing altitude nor any E–W or N–S trend to be observed. With respect to age and altitude, however, the two samples S of the Mesolcina valley indicate a slight increase in ages in the southernmost part of the nappe (Fig. 2).

Table 2 Apatite fission track data from the Adula nappe and selected adjacent units. For sample location, see Figure 2 and Table 1.

Sample No and Locality	Mineral and No. Crystals	Spontaneous ρ_S (N_S)	Induced ρ_i (N_i)	$P\chi^2$	Dosimeter ρ_d* (N_d)	Central FT Age (Ma) (-2σ/+2σ)	Mean Track Length	S.d. of distribution (No. Tracks)
MR P 214	apatite	0.004	0.156	64%	11.84	6.7	13.61	1.35 (51)
Solario	(20)	(46)	(1406)		(2886)	(-0.9/+1.1)		
MR P 220	apatite	0.002	0.048	74%	11.42	8.6	13.65	1.62 (55)
Vals	(40)	(38)	(863)		(2784)	(-1.3/+1.6)		
MR P 221	apatite	0.001	0.043	90%	11.35	5.0	13.59	1.51 (61)
Peil	(24)	(12)	(467)		(2767)	(-1.3/+1.7)		
MR P 222	apatite	0.012	0.313	80%	13.29	8.9	13.94	1.33 (100)
Guraletsch	(20)	(171)	(4376)		(4146)	(-0.7/+0.8)		
MR P 223	apatite	0.007	0.290	90%	11.28	4.8	13.40	1.50 (100)
Hinterrhein	(20)	(57)	(2292)		(2750)	(-0.6/+0.7)		
MR P 224	apatite	0.008	0.207	97%	11.21	7.1	13.86	1.63 (66)
San Bernardino	(20)	(32)	(865)		(2733)	(-2.1/+3.0)		
MR P 225	apatite	0.009	0.238	9%	11.14	7.2	13.70	1.61 (100)
Zapporthütte	(20)	(83)	(2215)		(2716)	(-0.9/+1.1)		
MR P 226	apatite	0.003	0.073	76%	11.07	6.8	13.71	1.11 (12)
Spina	(15)	(13)	(361)		(2699)	(-1.7/+2.2)		
MR P 227	apatite	0.010	0.372	91%	11.00	5.3	13.84	1.52 (24)
Pian San Giacomo	(20)	(42)	(1505)		(2682)	(-0.8/+0.9)		
MR P 228	apatite	0.004	0.166	57%	10.93	4.6	13.33	1.53 (76)
Castello Mesocco	(20)	(21)	(859)		(2665)	(-0.9/+1.1)		
MR P 258	apatite	0.004	0.114	91%	10.87	6.5	14.20	1.26 (100)
Lambertschalp	(20)	(32)	(916)		(2648)	(-1.1/+1.3)		
MR P 263	apatite	0.032	0.345	18%	10.66	16.9	13.27	1.65 (100)
Splügenpass	(20)	(281)	(3025)		(2598)	(-1.2/+1.3)		
MR P 264	apatite	0.004	0.419	60%	10.59	5.8	13.18	1.89 (100)
Soazza	(20)	(39)	(1218)		(2581)	(-0.9/+1.0)		
MR P 265	apatite	0.011	0.360	79%	10.52	5.5	13.95	1.48 (100)
Norantola	(20)	(98)	(3230)		(2564)	(-0.6/+0.6)		
MR P 266	apatite	0.006	0.132	69%	10.45	7.7	14.04	1.31 (59)
Alpe Arami	(20)	(38)	(885)		(2547)	(-1.2/+1.4)		
MR P 267	apatite	0.012	0.434	76%	10.38	4.8	14.15	1.56 (100)
Trescolmen	(20)	(107)	(3952)		(2530)	(-0.5/+0.5)		
MR P 268	apatite	0.001	0.059	13%	10.31	3.8	13.62	1.78 (37)
Pian d'As	(28)	(10)	(504)		(2513)	(-1.1/+1.5)		
MR P 269	apatite	0.018	0.597	100%	10.24	5.4	13.70	1.46 (100)
Cauco	(20)	(117)	(3842)		(2496)	(-0.5/+0.5)		
MR P 273	apatite	0.008	0.151	98%	10.17	9.0	13.20	1.65 (58)
Alpe di Lesgiüna	(20)	(60)	(1159)		(2479)	(-1.1/+1.3)		
MR P 275	apatite	0.002	0.062	80%	10.10	6.7	13.27	1.38 (52)
Alpe di Piotta	(20)	(20)	(520)		(2462)	(-1.4/+1.7)		
MR P 310	apatite	0.005	0.067	92%	9.542	11.2	13.93	1.34 (100)
Sass della Vacca	(20)	(35)	(514)		(2326)	(-1.8/+2.2)		
MR P 311	apatite	0.007	0.137	89%	9.612	8.1	14.28	1.30 (100)
Cima della Stagn	(20)	(64)	(1303)		(2343)	(-1.0/+1.1)		

(i) Track densities are ($\times 10^7$tr cm^{-2}), *=($\times 10^5$ tr cm^{-2}), numbers of tracks counted (N) shown in brackets;
(ii) Analyses by external detector method using 0.5 for the $4\pi/2\pi$ geometry correction factor;
(iii) Ages calculated using dosimeter glass CN-5 for apatite with ζ_{CN5} =344 ± 5;
(iv) P(χ^2) is probability for obtaining χ^2 value for ν degrees of freedom, where ν = no. crystals – 1;
(v) Track length data are given in 10^{-6} m, S.d. = 1σ standard deviation.

Mean FT lengths vary between 13.2 and 14.3 μm (Fig. 3), indicating monotonous cooling across the entire apatite partial annealing zone (APAZ). Track length distributions are narrow with a more or less prominent tailing towards shorter track lengths as a result of track formation during APAZ crossing (shortened tracks) and afterwards (tracks of full length). For the southern-

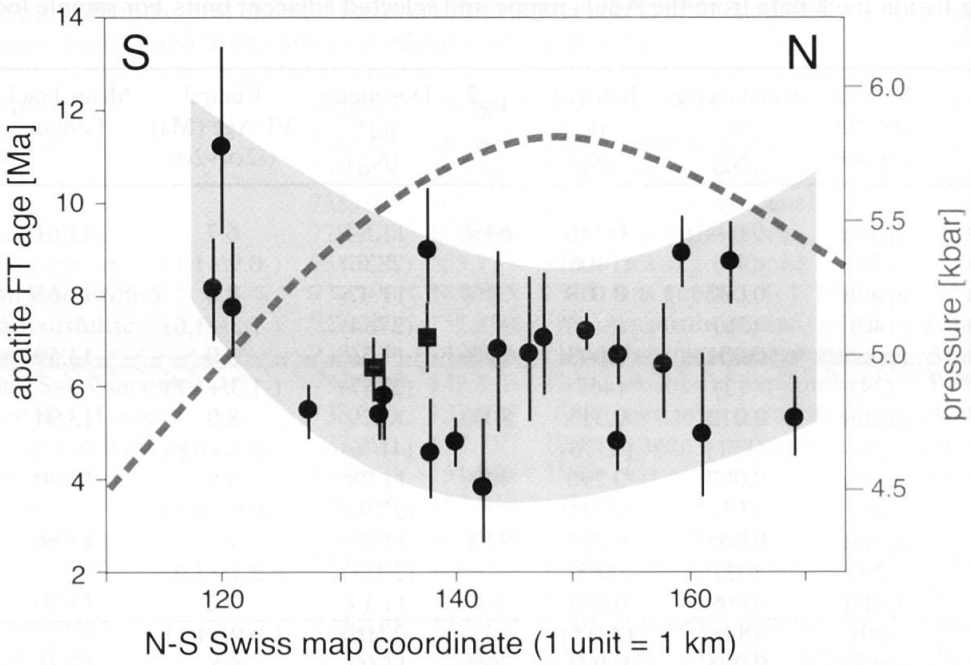

Fig. 4 Apatite fission track ages projected onto a N–S profile across the crystalline nappe body of the Adula nappe (with grey envelope) and metamorphic maximum palaeopressures as derived from the pressure contours based on mineral parageneses in Mesoalpine metamorphic sediments (taken from Todd and Engi, 1997). The pressure contour is here taken as a proxy for the total exhumation since the thermal peak of the Barrovian metamorphism. Squares: data from Wagner et al. (1977), dots: data from this study. Indicated age errors are 1σ.

most samples, mean track lengths are all around 14 μm (inset in Fig. 3). For the Splügen pass sample, the measured mean track length is identical to the mean track length of a formerly published sample (Hunziker et al., 1992).

3. Discussion

3.1. No late tilting but buckling

FT apatite ages from the Adula nappe do not show any significant age gradient in either E–W or N–S direction that may point to late tilting of the nappe due to e.g. regional updoming of the Lepontine dome to the W or as a result of ongoing enhanced exhumation along the Insubric line (Hurford, 1986) or a combination of these processes. Based on the E–W age distribution, the Adula nappe has not undergone any large-scale deformation after closure of the apatite FT system. At that time, the formerly S dipping geometry consistent with the PT data of the eclogite occurrences (Dale and Holland, 2003, proposed a 45° dip angle) and the PT-field gradient of the subsequent Barrovian overprint (Todd and Engi, 1997) had already changed into the flat lying geometry observed today (Fig. 1b). For the Ticino culmination, Steck and Hunziker (1994) indicate very rapid cooling after 22 Ma, but such doming must have stopped prior to the cooling of the Adula nappe to below 110 °C. The apatite ages in the Adula nappe are similar in range to ages observed along the Ticino valley (Wagner et al., 1977; Timar-Geng et al., 2004) or the Maggia valley (Hurford, 1986) further W. It is therefore concluded that the Adula nappe has not undergone any E–W or N–S tilting after 10 Ma and the eastern Lepontine dome has not experienced any significant regional doming with E–W exhumation gradient after that time.

The coincidence of relatively old ages and very long tracks for the southernmost samples can be attributed to a period of rapid cooling around 10 Ma, followed by a decrease in cooling rate, i.e. a concave shaped time-temperature path for the southernmost study area. Elevated exhumation along the Insubric line at around 10 Ma is in agreement with the data pattern observed further W, where Hurford (1986) reported similar apatite FT ages that show a slight age increase towards and across the Centovalli line and towards the Insubric line. In the Adula nappe data set, these slightly older ages in the S coincide with the longest mean track length data (inset in Fig. 3) indicating rather rapid cooling through the APAZ and slower cooling afterwards. This signal is interpreted to indicate a restricted zone of enhanced exhumation along the Insubric line at around 10 Ma. It is interesting to note that the pattern of the Adula

apatite FT ages is opposite to the pattern observed for the Rb–Sr biotite ages (Steck and Hunziker, 1994), where ages are similar along most of the N–S extension of the Adula nappe, but become younger in the southernmost part of the Adula nappe, indicating increased cooling between 20 and 10 Ma within the southernmost part of the nappe. The apatite FT data presented here illustrate that enhanced cooling (suggested to be the result of a thermal quench against the cold Southern Alpine block) along the Insubric line only stopped after 10 Ma.

Data on maximum metamorphic conditions reached during the Barrovian overprint show a marked increase of maximum temperatures from mid greenschist facies conditions at the front of the Adula nappe (near Vals, Fig. 1) to upper grade amphibolite facies in the South (Todd and Engi, 1997; Frey and Ferreiro-Mählmann, 1999). Pressure conditions recorded for this regional metamorphic overprint show a maximum close to 6.0 kbar in the central area of the Adula nappe, while pressures decrease towards N and S (Todd and Engi, 1997). These pressures need not represent a contemporaneous data pattern, but may have been recorded at different times. Nevertheless, they can be taken as a measure for the total exhumation that the rocks have experienced since metamorphism. If the maximum pressures reached in the Adula nappe are compared to the apatite age distribution, it is observed that the area of the highest recorded pressures during regional metamorphic overprint coincides with the central area of youngest apatite ages (Fig. 4). This coincidence suggests that the young apatite ages are the result of late differential exhumation, which was more pronounced in the central part than further N and S. As a result, it may be assumed that the late-stage evolution had a distinct influence on the present-day pattern of metamorphic maximum pressures in the Eastern Lepontine dome. The young ages in this middle part suggest also that the present-day flat-lying geometry of the nappe in N–S profiles (Fig. 1b) is a relatively young feature and the nappe had a more concave shape prior to this last event of differential exhumation. The observed age decrease in the middle Adula nappe would suggest a large-scale buckling with an E–W fold axis to be present in the eastern Lepontine dome.

3.2. Normal faulting between Adula and Tambo nappe

While the preceding discussion only deals with the N–S trend of the ages, it does not explain the E–W variation in apatite FT ages, which is evident across the Adula nappe and its adjacent units (Fig. 2). While apatite ages along the Mesolcina valley vary between 5 and 7 Ma (Fig. 2), with no age difference between the top of the Adula unit and the basis of the Tambo nappe (i.e. across the Misox zone), ages at the top of the Tambo and at the basis of the Suretta nappe (Splügen zone) are 10–17 Ma, as they are within the Tambo and Suretta nappes (Wagner et al., 1977; Hunziker et al., 1992). Thus, the apatite ages along the nappe-separating sediment zones suggest that there has been no vertical displacement since about 7 Ma along the Forcola zone, and since about 15 Ma along the Splügen zone.

On the other hand, the clear age difference between the basis and top of the Tambo nappe suggests that the rocks along the sediment zones have undergone different cooling histories, and that such differences in exhumation were arranged by normal faulting, which preferably took place along the sediment zones. The fact that the basal Tambo nappe yields an apatite age similar to samples from the top of the Adula unit is best interpreted by the influence of local shear heating or heat transfer from the footwall into the hanging wall over short distances. In such a scenario, the Tambo nappe basis would have undergone reheating during normal faulting by the juxtaposition of relatively colder Tambo rocks to the hotter Adula nappe top. The Suretta and Tambo nappe fission track data, however, appear to have had similar cooling histories, i.e. they acted as a coherent tectonic block that cooled through the APAZ during the Middle Miocene. Accordingly, the northern extension of the Forcola fault, assumed to follow the Misox zone (Meyre et al., 1998), remained active under brittle conditions during the Upper Miocene (i.e. much later than the suggested time range for the Forcola phase sensu Meyre et al., 1998), while no normal faulting occurred at that time in the Splügen zone. If, indeed, the Forcola zone was structurally linked to the Misox zone in the recent past, the evidence presented here should also be visible along the Forcola zone further S. Such a structural link has yet to be verified by signs of late brittle deformation and more FT data along the Forcola line.

3.3. Valley incision and evolution of the water divide

Apart from the regional age trends, apatite FT ages for the Adula unit reveal local age differences that do not fit into the regional pattern and cannot be explained by the differences in sampling altitude (375–2290 m, Table 1). A reasonable age-altitude correlation exists for the southern sam-

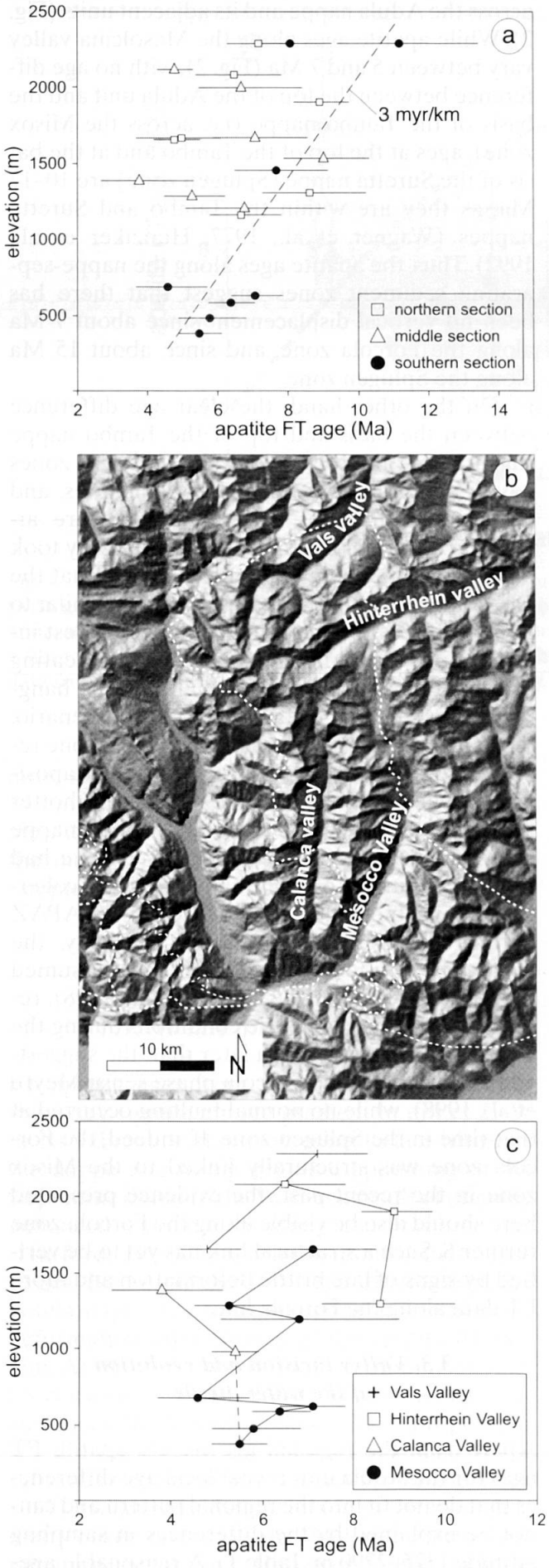

Fig. 5

ples only, while in the central and frontal part, age-altitude relationships are not systematic (Fig. 5a). Based on the age-altitude relationship in the S (3 myr/km), the variation in sampling altitude would account for a general age variation of 6 myr between valley bottom and the uppermost samples. However, most local age distributions show more complex patterns. The lack of a simple age-altitude relationship suggests a significant disturbance of the isothermal surfaces as a result of the past and present topography (Fig. 5b).

Disturbance of the near-surface isothermal surfaces is not only the result of the amplitude and wavelength of topography (Stüwe et al., 1994; Mancktelow and Grasemann, 1997), but also by dynamic changes of the topography (Stüwe and Hintermüller, 2000). The present-day topographic pattern of the Adula area is characterized by a small number of main valleys and a larger number of side valleys. The main valleys dissecting the Adula nappe are the Mesolcina, Vals, Hinterrhein and Calanca valley (Fig. 5b), and most samples were taken along the bottom of these valleys. In two major valleys, a transition from sedimentation-dominated to erosion-dominated valley bottoms is observed, which for the Hinterrhein valley coincides with the transition from the Northpenninic Bündnerschiefer to the Adula nappe crystalline rocks.

The upper Mesolcina valley follows the sediment zone between Adula and Tambo nappe. For this part of the valley it can be assumed that the position of the valley was defined by the different erodibility of the Bündnerschiefer and the crystalline rocks of adjacent nappes. It is thus likely that, in time, the E–W position of the upper Mesolcina valley has shifted to the E owing to the dip of the sediment zone, which was caused earlier by the formation of the Lepontine Dome (Timar-Geng et al., 2004). The neighbouring Calanca valley, in contrast, is not bound by any tectonically or lithologically given direction. Owing to its ero-

Fig. 5 (a) Apatite fission track ages (with 1σ errors) for the Adula unit, sorted according to a rough division into a southern, middle and northern nappe section. Only for the southern nappe section, a moderate age-altitude correlation (dashed line $R^2 = 0.7$) reveals a common cooling history and a rather stable evolution of the isothermal planes. (b) Digital elevation model of the Alps around the outline of the Adula nappe (white dashed line) and indicated main valleys entering the crystalline nappe body. (c) Apatite fission track ages (with 1σ errors) versus sampling altitude along the four main valleys as indicated in Figure 5b. A dashed line at the southern end of the Calanca valley data set indicates its erosional basis in the Mesolcina valley.

sional basis within the Mesolcina valley, the Calanca valley's evolution depended on the evolution of the Mesolcina valley.

It is interesting to note that the Mesolcina valley does not follow the highly erodible Northpenninic Bündnerschiefer, which run across San Bernardino pass. Instead the valley cuts through crystalline rocks of the Adula and Simano nappes, which are more resistant to erosion (Kühni and Pfiffner, 2001) and whose fold axes and main schistosity run approximately normal to the valley direction (Nagel et al., 2002). The evolution of the valley must have been influenced by other processes, e.g. regional exhumation. The following scenario is an attempt to bring geomorphologic considerations and the evidence of exhumation presented here into a consistent model.

Kühni (1999) proposed that the water divide in the Alpine belt migrated substantially northwards as a result of increased exhumation of the central massifs N of the Lepontine dome. During strong backfolding (30–25 Ma, Nagel et al., 2002, until 19 Ma according to Schmid et al., 1996) the water divide in the central Alps was located slightly north to the Insubric Line and the Bergell intrusives, but shifted further N due to increased tectonic stacking and exhumation of the Aar massif and the Gotthard nappe after 20 Ma (Schmid et al., 1996). Such a scenario would lead to a strong deepening and backward migration of the valleys in the Ticino area between the former and the new water divide. In some valleys, flow direction would be changed to the opposite direction.

In such a setting, the lower Mesolcina valley, being a tributary to the Ticino main valley, would have grown considerably deeper and erode backwards and eventually reach into the sediment zone between Adula and Tambo nappe, from where river erosion would be guided towards N, into a valley that previously existed due to the higher erodibility of the sediments in-between the two crystalline nappes.

Based on observations in the Napf detrital fan and geomorphological considerations, Hantke (1984) proposed a shift in the water divide as late as the younger Miocene. Modelling results (Kühni, 1999) suggest that within about 10 myr the drainage pattern within the central Alps would have adapted to the new situation with a shift of the water divide into the area of the present-day outcrops of the Aar and Gotthard massifs, leading to an inversion in river flow direction in the upper Mesolcina valley. Such a scenario is in line with observations of strong post-late Oligocene valley incisions within neighbouring valleys to the E (Hantke, 1984). The formation and evolution of the present-day Calanca valley (a tributary to the Mesolcina valley) required such an erosional break-through of the Mesolcina valley to the SW and would have mainly developed after 10 Ma.

Given the different erodibility of the geologic units and the pronounced relief of the upper Mesolcina valley, it seems likely that this valley has existed and influenced the isothermal surfaces for a long time, whereas the Calanca valley has evolved more recently. A comparison of valley bottom ages between the different valleys across the Adula nappe (Fig. 5c) reveals that the southernmost age along the Calanca valley corresponds to ages at the erosional basis in the Mesolcina valley, but the age upstream in the Calanca valley is distinctly younger. This points to backward erosion, where cooling of the valley bottom rocks is influenced not only by vertical incision, but also by horizontal backward erosion. For the Mesolcina valley, FT ages are rather constant, as is typical for a mature valley with constant vertical erosion rates along stream. For the Hinterrhein valley, a young age is found downstream of a marked change in slope, where the valley enters the crystalline rocks of the Adula nappe, while a sample close to the spring of the Hinterrhein (and at higher altitude) is distinctly older. Along the Vals valley, ages are relatively old, with the exception of the uppermost sample closest to the river spring, which is distinctly younger and may again be interpreted as the result of recent backward erosion in the valley. Thus, based on to their valley bottom FT ages and the age variation along stream, the upper Mesolcina valley and the lower Vals valley may be considered older and mature valleys, while the Calanca, Hinterrhein and uppermost Vals valleys are interpreted as a younger generation of valleys that has continued to propagate upstream in the recent past. Because the samples along the lower Mesolcina valley and the nearby slopes dominate the sample set in the southern Adula nappe, this part of the Adula unit fits a simple age-altitude relationship (Fig. 4a).

In summary, we suggest that the evolution of the water divide from a position north of the Insubric Line to within the Aar and Gotthard massifs between 20 and 10 Ma led to a change in river flow direction along the Misox zone and a strong incision of the lower Mesolcina valley. The Calanca and Hinterrhein valleys had to evolve accordingly, and their recent backward erosion is evident in the apatite FT data set.

4. Conclusions

The apatite FT age pattern of the Adula nappe reveals part of the late-stage cooling history of

this unit, which included both tectonic and erosional features.

– The absence of any simple E–W or N–S gradients in FT ages illustrates that the Adula nappe has not undergone any tilting later than closure of the apatite FT system as one coherent block, as may be suggested from the metamorphic gradients or the exhumation of the Lepontine dome to the W.

– The oldest ages and longest track length data in the S of the investigated area reveal a period of enhanced exhumation along the Insubric line, continuing until about 10 Ma ago.

– Youngest FT ages coincide with the highest pressures derived for mineral parageneses in Mesoalpine metamorphic sediments suggesting a moderate updoming in the central part of the nappe. It is proposed that this process has influenced the now exposed pressure pattern along the eastern Lepontine dome.

– The difference in apatite FT ages between the Misox zone and the Splügen zone is interpreted as the result of a late normal faulting between Adula and Tambo nappe, during which the Tambo nappe basis was reheated, and the apatite FT system was rejuvenated. Owing to the low data density within the Tambo nappe, it is not yet clear whether such normal faulting has extended S along the Forcola line.

– Samples taken along the major valleys entering or crossing the Adula nappe reveal differences in their cooling age patterns. Valleys with old and constant ages along stream (in particular the Mesolcina valley) are interpreted to represent topographic features that have persisted since the Middle Miocene. Other valleys show age differences near jumps in altitude (e.g. Calanca valley); these are interpreted as relatively young and backward migrating valleys. Their incision followed a major northward shift of the central Alpine water divide during the Miocene. FT samples taken along river beds can be therefore used to quantify the topographic evolution of regions showing sufficiently high relief.

Acknowledgements

This study was part of project Ra 704/3-1, which has been funded by the Deutsche Forschungsgemeinschaft (DFG). Two rock samples were provided by O. Jeker and J. Mullis. I owe thanks to D. Wiedenmann and N. Kindler for their help with mineral separation, to H. Fesenmeier and E. Aringer for preparation of the mineral mounts, and to D. Seward and B. Fügenschuh for allowing me to use their FT equipment at ETH Zürich and at University of Basel. Reviews by A. Berger and M. Engi pointed out additional important aspects and thus markedly improved the quality of the manuscript.

References

Becker, H. (1993): Garnet peridotite and eclogite Sm–Nd mineral ages from the Lepontine dome (Swiss Alps): New evidence for Eocene high-pressure metamorphism in the Central Alps. *Geology* **21**, 599–602.

Berger, A., Rosenberg, C. and Schmid, S.M. (1996): Ascent, emplacement and exhumation of the Bergell pluton within the Southern Steep Belt of the Central Alps. *Schweiz. Mineral. Petrogr. Mitt.* **76**, 357–382.

Berger, A., Mercolli, I. and Engi, M. (2005): The central Lepontine Alps: Notes accompanying the tectonic and petrographic map sheet Sopra Ceneri (1:100'000). *Schweiz. Mineral. Petrogr. Mitt.* **85**, 109–146.

Bucher-Nurminen, K. and Droop, G.T.R. (1983): The metamorphic evolution of garnet-cordierite-sillimanite gneisses of the Gruf-Complex, eastern Pennine Alps. *Contrib. Mineral. Petrol.* **84**, 215–227.

Ciancaleoni, L., Marquer, D. and Fügenschuh, B. (2001): Continental collision, extension, lateral extrusion and the timing of deformations in the internal domain of a mountain belt: an example from the Eastern Central Alps (Bergell area) during the Oligo-Miocene. EUG 11: EUGIX.G4.1381.

Dale, J. and Holland, T.J.B. (2004): Geothermobarometry, P–T paths and metamorphic field gradients of high-pressure rocks from the Adula nappe, Central Alps. *J. metamorphic Geol.* **21**, 813–829.

Engi, M., Berger, A. and Roselle, G. (2001): The role of the tectonic accretion channel (TAC) in collisional orogeny. *Geology* **29**, 1143–1146.

Frey, M. and Ferreiro-Mählmann, R. (1999): Alpine metamorphism of the Central Alps. *Schweiz. Mineral. Petrogr. Mitt.* **79**, 135–154.

Galbraith, R.F. and Laslett, G.M. (1993): Statistical models for mixed fission track ages. *Nucl. Tracks Rad. Meas.* **17**, 197–206.

Giger, M. and Hurford, A.J. (1989): Tertiary intrusives of the Central Alps: Their Tertiary uplift, erosion, redeposition and burial in the south-alpine foreland. *Ecl. geol. Helvetiae* **82**, 857–866.

Grasemann, B. and Mancktelow, N. (1993): Two-dimensional thermal modelling of normal faulting; the Simplon fault zone, Central Alps, Switzerland. *Tectonophysics* **225**, 155–165.

Hantke, R. (1984): Zur tertiären Relief- und Talgeschichte des Bergeller Hochgebirges, der zentralen Südalpen und der angrenzenden Gebiete. *Ecl. geol. Helvetiae* **77**, 327–361.

Heinrich, C. (1986): Eclogite Facies Regional Metamorphism of Hydrous Mafic rocks in the Central Alpine Adula Nappe. *J. Petrol.* **27**, 123–154.

Hunziker, J.C., Desmons, J. and Hurford, A.J. (1992): Thirty-two years of geochronological work in the Central and Western Alps: A review on seven maps. *Mém. Géologie (Lausanne)* **13**, 59 pp.

Hurford, A.J. and Green, P.F. (1983): The zeta age calibration of fission track dating. *Isotope Geosciences* **1**, 285–317.

Hurford, A.J. (1986): Cooling and uplift patterns in the Lepontine Alps, South Central Switzerland, and an age of vertical movement on the Insubric fault line. *Contrib. Mineral. Petrol.* **92**, 413–427.

Jenny, H., Frischknecht, G. and Kopp, J. (1923): Geologie der Adula. *Beitr. geol. Karte Schweiz* (N.F.) **51**, 1–123.

Kühni, A. (1999): Evolution of the topography and drainage network of the Swiss Alps in response to Late Tertiary compression and exhumation: Insights from large-scale analysis of a digital elevation model and numerical surface processes modelling. Unpubl. Ph.D thesis, Universität Bern, 123 pp.

Kühni, A. and Pfiffner, O.A. (2001): The relief of the Swiss Alps and adjacent areas and its relation to lithology and structure: topographic analysis from a 250-m DEM. *Geomorphology* **41**, 285–307.

Mancktelow, N.S. (1992): Neogene lateral extension during convergence in the Central Alps: evidence from inter-related faulting and backfolding around the Simplonpass (Switzerland). *Tectonophysics* **215**, 295–317.

Mancktelow, N. and Grasemann, B. (1997): Time-dependent effects of heat advection and topography on cooling histories during erosion. *Tectonophysics* **270**, 167–195.

Meyre, C., De Capitani, C. and Partzsch, J. (1997): A ternary solid solution model for omphacite and its application to geothermobarometry of eclogites from the Middle Adula nappe (Central Alps, Switzerland). *J. metamorphic Geology* **15**, 687–700.

Meyre, C., Marquer, D., Schmid, S.M. and Ciancaleoni, L. (1998): Syn-orogenic extension along the Forcola fault: Correlation of Alpine deformation in the Tambo and Adula nappes (Eastern Penninic Alps). *Ecl. geol. Helvetiae* **91**, 409–420.

Nagel, T., De Capitani, C., Frey, M., Froitzheim, N., Stünitz, H. and Schmid, S. (2002): Structural and metamorphic evolution during rapid exhumation in the Lepontine dome (southern Simano and Adula nappes, Central Alps, Switzerland). *Ecl. geol. Helvetiae* **95**, 301–321.

Nievergelt, P., Liniger, M., Froitzheim, N. and Ferreiro-Mählmann, R. (1996): Early to mid Tertiary crustal extension in the Central Alps: The Turba Mylonite Zone (Eastern Switzerland). *Tectonics* **15**, 329–340.

Niggli, E. (1970): Alpine Metamorphose und Alpine Gebirgsbildung. *Fortschritte der Mineralogie* **47**, 16–26.

Roselle, G.T., Thüring, M. and Engi, M. (2002): MELONPIT: a finite element code for simulating tectonic mass movement and heat flow within subduction zones. *Am. J. Sci.* **302**, 381–409.

Schlunegger, F. and Willett, S.D. (1999): Spatial and temporal variations in exhumation of the central Swiss Alps and implications for denudation mechanisms. In: Ring, U., Brandon, M.T., Lister, G.S., Willett, S.D. (eds.): Exhumation processes: normal faulting, ductile flow and erosion. *Geol. Soc. London Spec. Publ.* **154**, 157–180.

Schmid, S.M., Rück, P. and Schreurs, G. (1990): The significance of the Schams nappes for the reconstruction of the paleotectonic and orogenic evolution of the Penninic zone along the NFP-20 East traverse (Grisons, eastern Switzerland). *Mém. Soc. géol. France* **156**, 263–287.

Schmid, S.M., Pfiffner, O.A., Froitzheim, N., Schönborn, G. and Kissling, E. (1996): Geophysical-geological transect and tectonic evolution of the Swiss-Italian Alps. *Tectonics* **15**, 1036–1064.

Steck, A. and Hunziker, J. (1994): The Tertiary structural and thermal evolution of the Central Alps – Compressional and extensional structures in an orogenic belt. *Tectonophysics* **238**, 229–254.

Steinmann, M.C. (1994): Die nordpenninischen Bündnerschiefer der Zentralalpen Graubündens: Tektonik, Stratigraphie und Beckenentwicklung. Unpubl. Ph.D thesis, ETH Zürich, Nr. 10668, 220 pp.

Stüwe, K. and Hintermüller, M. (2000): Topography and isotherms revisited: the influence of laterally migrating drainage divides. *Earth Planet. Sci. Lett.* **184**, 287–303.

Stüwe, K., White, L. and Brown, R. (1994): The influence of eroding topography on steady-state isotherms. Application to fission-track analysis. *Earth Planet. Sci. Lett.* **124**, 63–74.

Timar-Geng, Z., Grujic, D. and Rahn, M. (2004): Deformation at the Leventina-Simano nappe boundary, Central Alps, Switzerland. *Ecl. geol. Helvetiae* **97**, 265–278.

Todd, C.S. and Engi, M. (1997): Metamorphic field gradients in the Central Alps. *J. metamorphic Geology* **15**, 513–530.

Wagner, G.A., Reimer, G.M. and Jäger, E. (1977): Cooling ages derived by apatite fission-track, mica Rb–Sr and K–Ar dating: The uplift and cooling history of the Central Alps. *Mem. Ist. Geol. Mineral. Univ. Padova* **30**, 27 pp.

Wagner, G.A., Miller, D.S. and Jäger, E. (1979): Fission track ages on apatite of Bergell rocks from Central Alps and Bergell boulders in Oligocene sediments. *Earth Planet. Sci. Lett.* **45**, 355–360.

Received 21 April 2005
Accepted in revised form 22 May 2006
Editorial handling: M. Engi